

# Absorbing boundary conditions for the Schrödinger equation on finite intervals

J.-P. Kuska

*Institut für Ionen- und Elektronenphysik, Humboldt-Universität zu Berlin, Fachbereich Physik,  
Invalidenstrasse 110, O-1040 Berlin, Germany*

(Received 22 January 1992; revised manuscript received 6 April 1992)

The absorbing boundary conditions for the one- and two-dimensional Schrödinger equation on a finite interval are considered by using a rational-function approximation for the dispersion relation. The approximation gives good results over a wide range of input parameters. A finite-difference approximation is used to solve the Schrödinger equation and the resulting boundary conditions.

## I. INTRODUCTION

The pure numerical solution of the time-dependent Schrödinger equation in low-dimensional systems was used first by Goldberg, Schey, and Schwartz<sup>1</sup> to generate motion pictures of a one-dimensional quantum particle. Traditionally the treatment of quantum scattering events is to expand the wave function into a set of traveling waves. The traveling waves obey the boundary conditions implicitly. With the growing interest of transport properties of low-dimensional quantum devices, pure numerical techniques for solving the Schrödinger equation have become more important.

The one-dimensional Schrödinger equation

$$i\hbar \frac{\partial \psi}{\partial t}(x, t) = -\frac{\hbar^2}{2m} \frac{\partial^2 \psi}{\partial x^2}(x, t) + V(x)\psi(x, t) \quad (1)$$

describes the motion of a particle with the mass  $m$  in the interval  $x \in (-\infty, \infty)$  under the influence of the potential  $V$ . The boundary conditions on the infinite interval are implied by the normalization condition

$$\int_{-\infty}^{\infty} \psi^*(x, t)\psi(x, t) dx = 1, \quad \forall t.$$

In the two-dimensional case, one has the similar expressions

$$i\hbar \frac{\partial \psi}{\partial t}(x, y, t) = -\frac{\hbar^2}{2m} \left( \frac{\partial^2 \psi}{\partial x^2}(x, y, t) + \frac{\partial^2 \psi}{\partial y^2}(x, y, t) \right) + V(x, y)\psi(x, y, t), \quad (2)$$

$$\int_{-\infty}^{\infty} \int_{-\infty}^{\infty} \psi^*(x, y, t)\psi(x, y, t) dx dy = 1, \quad \forall t$$

with  $x, y \in [-\infty, \infty]$ . The pure numerical solution of Eq. (2) was given by Galbraith, Ching, and Abraham in Ref. 2. The numerical solution of (1) or (2) by finite-difference or finite-element techniques can only be performed on a finite interval. The problem there is to choose appropriate boundary conditions in a way that the finiteness of the interval has a minor influence to the

solution of (1) or (2) inside the interval. One way is to choose  $\psi = 0$  at the boundary. This condition works well for the case that the particle is far from the boundaries. For long times and close to the boundaries, reflections occur. To avoid these reflections several techniques were supposed; for a review see Frensky.<sup>3</sup> Shibata<sup>4</sup> made an approach to design absorbing boundary conditions for the one-dimensional case. The present work will give a better approximation for the boundary conditions in one dimension and present boundary conditions for the two-dimensional case in Sec. II and show some numerical results in Sec. III.

## II. HIGHLY ABSORBING BOUNDARY CONDITIONS

### A. One-dimensional case

This section follows the ideas developed in Refs. 5 and 4. To construct absorbing boundary conditions, the boundary should be almost transparent for a plane wave of the form

$$\psi(x, t) = \exp[-i(\omega t - kx)]. \quad (3)$$

Due to this assumption the expressions are only valid for scattering states. The idea is to construct an algebraic equation for the wave vector  $k$  and the frequency  $\omega$  and then to use the correspondence between the  $x$ - $t$  space and the  $k$ - $\omega$  space to construct a differential equation on the boundaries which is transparent for the plane waves. It is clear that it is impossible to design fully absorbing boundary conditions. From (1) and (3) one gets the dispersion relation for the wave vector  $k$ ,

$$\hbar^2 k^2 = 2m[\hbar\omega - V(x)]. \quad (4)$$

This relation can be solved for  $k$  and yields

$$\hbar k = \pm \sqrt{2m[\hbar\omega - V(x)]}, \quad (5)$$

where the plus sign describes waves moving to  $x = \infty$  and the minus sign means waves moving to  $x = -\infty$ . The left boundary has to be transparent for left-going waves and the right boundary must be transparent for right-going waves. To transform (5) back into the  $x$ - $t$  space

one needs an approximation for the square root which can be easily transformed into a differential equation at the boundaries.

In Ref. 4 a linear approximation of the square root function is used. The linear approximation introduces two unphysical parameters into the calculation and it is difficult to choose the right values. In the present paper the rational function approximation

$$\sqrt{z - z_0} \approx \sqrt{z_0}(1 + 3z/z_0)/(3 + z/z_0) \quad (6)$$

is used.

With the approximation (6) for the square root in the dispersion relation (5) one gets

$$\hbar k = \pm \hbar k_0 \left[ \frac{2m(\hbar\omega - V)}{\hbar^2 k_0^2} \right]^{1/2} \approx \pm \hbar k_0 \frac{1 + 3z}{3 + z} \quad (7)$$

with  $z = 2m(\hbar\omega - V)/\hbar^2 k_0^2$ .  $k_0$  plays the role of the expansion point in the rational function approximation (5). The mean wave vector of the localized wave function is still unknown when it arrives at the boundary. One has to choose a value for  $k_0$  in such a way that the boundary is transparent for the incoming wave packet. By using the correspondence between  $k \iff -i\partial/\partial x$ ,  $\omega \iff i\partial/\partial t$  one gets the partial differential equation

$$\begin{aligned} -i\hbar \left( 3 \frac{\hbar^2 k_{0x}^2}{2m} - V \right) \frac{\partial \psi}{\partial x}(x, y, t) + \hbar^2 \frac{\partial^2 \psi}{\partial t \partial x}(x, y, t) - i \frac{\hbar^3}{2m} \frac{\partial^3 \psi}{\partial y^2 \partial x}(x, y, t) \\ = \pm \hbar k_{0x} \left( \frac{\hbar^2 k_{0x}^2}{2m} - 3V \right) \psi(x, y, t) \pm 3i\hbar^2 k_{0x} \frac{\partial \psi}{\partial t}(x, y, t) \pm 3 \frac{\hbar^3 k_{0x}}{2m} \frac{\partial^2 \psi}{\partial y^2}(x, y, t). \end{aligned} \quad (11)$$

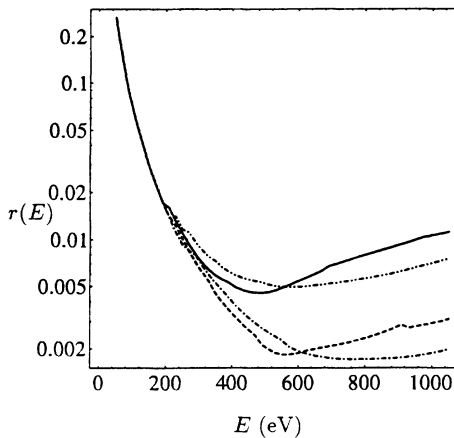


FIG. 1. The reflection coefficient  $r$  vs the energy (eV) of the particle for different time steps  $\delta$  and grid sizes  $J$ . The solid line refers to  $\delta = 1.0 \times 10^{-4}$  and  $J = 512$ , the dotted-dashed-dotted line refers to  $\delta = 0.5 \times 10^{-4}$  and  $J = 512$ , the dashed line was obtained with  $\delta = 1.0 \times 10^{-4}$  and  $J = 1024$ , and the dashed-dotted line with  $\delta = 0.5 \times 10^{-4}$  and  $J = 1024$ .

$$\begin{aligned} -i\hbar \left( 3 \frac{\hbar^2 k_0^2}{2m} - V \right) \frac{\partial \psi}{\partial x}(x, t) + \hbar^2 \frac{\partial^2 \psi}{\partial t \partial x}(x, t) \\ = \pm \hbar k_0 \left( \frac{\hbar^2 k_0^2}{2m} - 3V \right) \psi(x, t) \pm 3i\hbar^2 k_0 \frac{\partial \psi}{\partial t}(x, t). \end{aligned} \quad (8)$$

### B. Two-dimensional case

The two-dimensional case in Eq. (2) can be treated in a similar way. Only the derivation in the  $x$  direction will be given. The expressions for the  $y$  direction can be obtained by exchanging  $x$  with  $y$ .

The two-dimensional plane wave can be expressed by

$$\psi(x, y, t) = \exp[-i(\omega t - k_x x - k_y y)], \quad (9)$$

where  $k_x$  is the wave vector in the  $x$  direction and  $k_y$  is the wave vector in the  $y$  direction. The expansion point of the dispersion relation may be  $\mathbf{k}_0 = (k_{0x}, k_{0y})$ . The dispersion relation yields

$$\hbar k_x = \pm \hbar k_{0x} \{ [2m(\hbar\omega - V) - \hbar^2 k_y^2] / \hbar^2 k_{0x}^2 \}^{1/2}. \quad (10)$$

Using again the approximation (6) for the argument of the square root function yields the boundary conditions

At  $x = 0$  the minus sign should be used and at  $x = L$  the plus sign.

## III. NUMERICAL RESULTS

For the numerical solution of Eq. (1) with the boundary conditions (8) and Eq. (2) with the boundary conditions (11),  $\hbar = 1$ ,  $m = \frac{1}{2}$ , and  $L = 10 \text{ \AA}$  are chosen. The potential  $V$  was set to  $V = 0$ .

### A. One-dimensional case

As initial wave function a wave packet

$$\psi(x, 0) \propto \exp[-(x - \xi)^2 / 2\sigma_0] \exp(iqx)$$

was chosen. Equations (1) and (8) were approximated by a finite-difference approximation. For the details of the approximation of the Schrödinger equation on the inner points, see Refs. 1 and 2. The abbreviations  $x_j = j\epsilon$  with  $j = 0, \dots, J$ ,  $t_n = n\delta$  with  $n = 0, \dots, N$  and  $\psi(x_j, t_n) = \psi_j^n$  are used in the notation of the finite-difference equations. On the boundaries the finite-difference approximations at  $x = 0$  ( $j = 0$ ) and  $x = L$

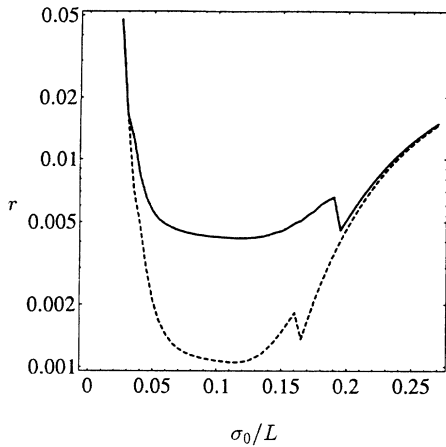


FIG. 2. The reflection coefficient  $r$  vs the initial width  $\sigma_0/L$  of the wave packet with an energy of 650 eV. The solid line shows the results for  $\delta = 0.5 \times 10^{-4}$  and  $J = 512$  and the dashed line shows the dependence for  $\delta = 0.5 \times 10^{-4}$  and  $J = 1024$ .

$$(j = J - 1)$$

$$\begin{aligned} \psi(x, t) &\approx \frac{1}{4} (\psi_{j+1}^{n+1} + \psi_j^{n+1} + \psi_{j+1}^n + \psi_j^n), \\ \frac{\partial \psi}{\partial x}(x, t) &\approx \frac{1}{2\epsilon} (\psi_{j+1}^{n+1} - \psi_j^{n+1} + \psi_{j+1}^n - \psi_j^n), \\ \frac{\partial \psi}{\partial t}(x, t) &\approx \frac{1}{2\delta} (\psi_{j+1}^{n+1} + \psi_j^{n+1} - \psi_{j+1}^n - \psi_j^n), \\ \frac{\partial^2 \psi}{\partial t \partial x}(x, t) &\approx \frac{1}{\epsilon \delta} (\psi_{j+1}^{n+1} - \psi_j^{n+1} - \psi_{j+1}^n + \psi_j^n) \end{aligned}$$

are used. This yields the usual tridiagonal system of equations for the calculation of the  $\psi_j^{n+1}$ .

To prove the quality of the absorbing boundary conditions for various energies of the moving particle, the reflection coefficient

$$r = \frac{\int_0^L \psi^*(x, t_N) \psi(x, t_N) dx}{\int_0^L \psi^*(x, 0) \psi(x, 0) dx}$$

was calculated. The particle was located around  $\xi = 3L/4$  at  $t = 0$  moving in a positive  $x$  direction. The width of the wave function  $\sigma_0$  was set to 5% of  $L$ . The expansion point  $k_0$  of the approximation (6) was set to  $k_0 = q$ . The value  $t_N > 0$  was determined by the relation

$$\int_0^L x \psi^*(x, t_N) \psi(x, t_N) dx / \int_0^L \psi^*(x, 0) \psi(x, 0) dx < \xi.$$

The results of this calculation are shown in Fig. 1. As is seen from Fig. 1 a reflection coefficient less than 1% or better is easily obtained for a wide range of energies. The variation of the step size of time integration has a small influence on the quality of the boundary conditions. A larger number of mesh points gives significantly better results. For low energies of the particle the diffusionlike motion dominates the particle flux out of the interval. The boundary condition is not designed for that case and yields bad results.

In Fig. 2 the dependence of the reflection coefficient  $r$  on the width of the wave packet is shown. Narrow wave packets (small  $\sigma_0$ ) correspond to relatively wide wave packets in the  $k$  space and give relatively bad results (even less than 5%). For  $\sigma_0 > 0.13L$  the wave packet

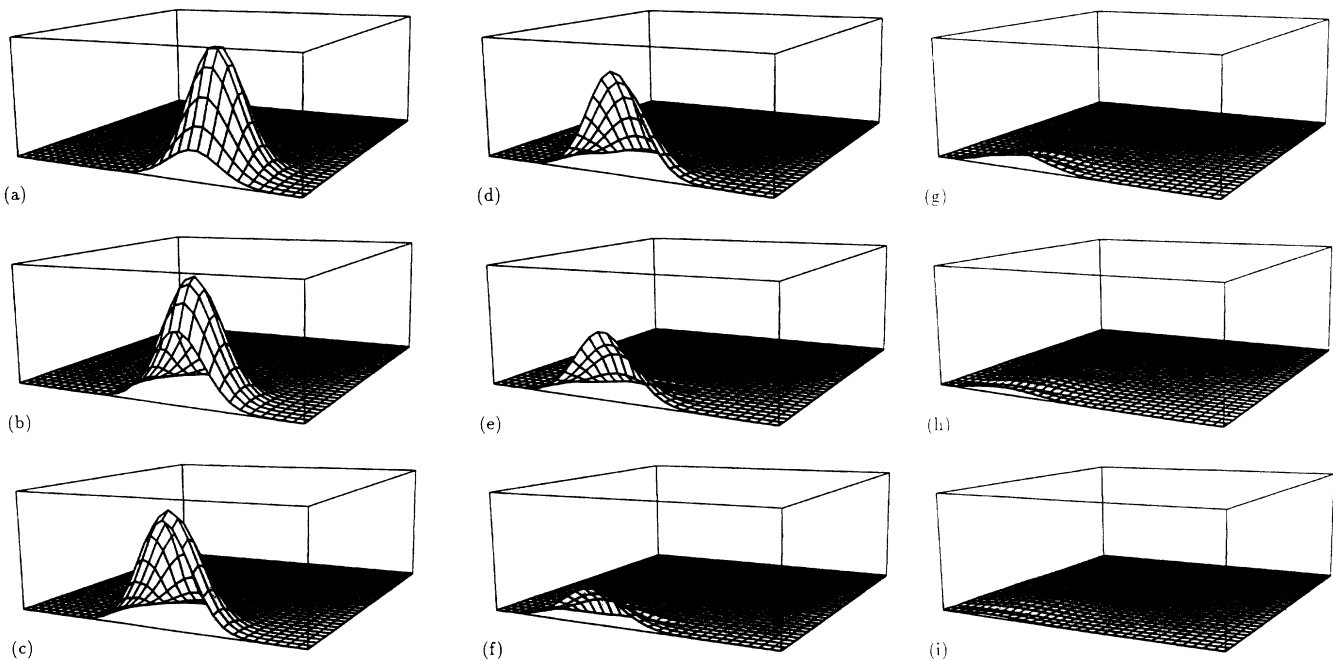


FIG. 3. Two-dimensional motion of a particle on a  $128 \times 128$  grid with energy of 400 eV and  $q_x = q_y = q$ .  $|\psi(x, y, t)|$  is drawn for  $n = 80$  (a), to  $n = 400$  (i). Between the pictures are always 40 time steps of width  $\delta = 1.0 \times 10^{-5}$ .  $k_{0x} = k_{0y} = k_0 = 3.1q$  were taken as parameters for the boundary conditions.

will not fit in the interval any longer and the results also become bad.

### B. Two-dimensional case

For the two-dimensional case an initial wave packet of the form

$$\psi(x, y, 0) \propto \exp\{-(x - \xi_x)^2 + (y - \xi_y)^2 / 2\sigma_0\} \times \exp[i(q_x x + q_y y)]$$

was used. The inner points of (2) were treated as suggested in Ref. 2. To transform Eq. (11) into a finite-difference expression the approximations

$$\psi(x, y, t) \approx \frac{1}{4}(\psi_{j+1,l}^{n+1} + \psi_{j+1,l}^n + \psi_{j,l}^{n+1} + \psi_{j,l}^n),$$

$$\frac{\partial \psi}{\partial x}(x, y, t) \approx \frac{1}{2\epsilon}(\psi_{j+1,l}^{n+1} - \psi_{j,l}^{n+1} + \psi_{j+1,l}^n - \psi_{j,l}^n),$$

$$\frac{\partial \psi}{\partial t}(x, y, t) \approx \frac{1}{2\delta}(\psi_{j+1,l}^{n+1} - \psi_{j+1,l}^n + \psi_{j,l}^{n+1} - \psi_{j,l}^n),$$

$$\frac{\partial \psi}{\partial t \partial x}(x, y, t) \approx \frac{1}{\epsilon \delta}(\psi_{j+1,l}^{n+1} - \psi_{j+1,l}^n - \psi_{j,l}^{n+1} + \psi_{j,l}^n),$$

$$\frac{\partial^2 \psi}{\partial y^2}(x, y, t) \approx \frac{1}{2\epsilon^2}(\psi_{j+1,l+1}^n - 2\psi_{j+1,l}^n + \psi_{j+1,l-1}^n + \psi_{j,l+1}^n - 2\psi_{j,l}^n + \psi_{j,l-1}^n),$$

$$\frac{\partial^3 \psi}{\partial y^2 \partial x}(x, y, t) \approx \frac{1}{\epsilon^3}[(\psi_{j+1,l+1}^{n+1} - 2\psi_{j+1,l}^{n+1} + \psi_{j+1,l-1}^{n+1}) - (\psi_{j,l+1}^{n+1} - 2\psi_{j,l}^{n+1} + \psi_{j,l-1}^{n+1})]$$

are used with the abbreviations  $x_j = j\epsilon$ ,  $y_l = l\epsilon$ ,  $t_n = n\delta$  and  $\psi(x_j, y_l, t_n) = \psi_{j,l}^n$  where  $j = 0, J-1$ ,  $l = 0, \dots, J$  and  $n = 0, \dots, N$ . Similar expressions are used for the boundaries at  $y = 0$  and  $y = L$ . This yields again a large linear system for the  $\psi_{j,l}^{n+1}$ . To solve the resulting equations the alternating direction implicit (ADI) method of Ref. 2 is used. Due to the fact that ADI is not an implicit solution method the time step  $\delta$  must be chosen so that the following stability condition,

$$\max \left| \frac{-2a \pm 2d + i(4b \pm c)}{2a \pm 2d - 8e + i(4b \mp c \pm 4f)} \right| < 1,$$

with

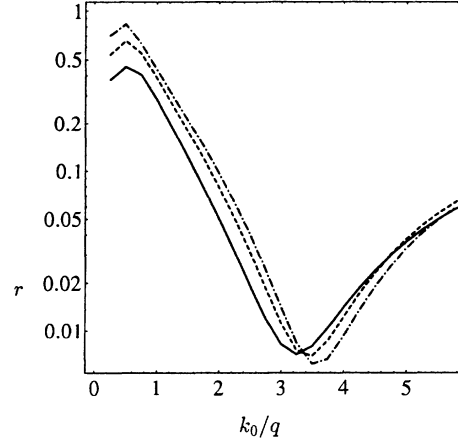


FIG. 4. Two-dimensional reflection coefficient  $r$  for the scattering event shown in Fig. 3 on a  $64 \times 64$  grid with  $\delta = 0.5 \times 10^{-4}$ ,  $k_0$  was varied in terms of  $q$  to change the transparency of the boundary. The solid line shows the  $r(k_0/q)$  dependence for a 200-eV particle, the dashed line for a particle with 300 eV energy, and the dashed-dotted line corresponds to a 400-eV particle.

$$\begin{aligned} a &= (\hbar/\epsilon)(3\hbar^2 k_0^2/2m - V), & b &= \hbar^2/\epsilon\delta, \\ c &= \hbar k_0(\hbar^2 k_0^2/2m - 3V), & d &= 3\hbar^2 k_0/\delta, \\ e &= (1/\epsilon^3)(\hbar^3/2m), & f &= (3\hbar k_0/\epsilon^2)(\hbar^2/2m) \end{aligned}$$

is fulfilled for  $k_0 = k_{0x}$  and  $k_{0y}$ .

Figure 3 shows the motion of a quantum particle with 400 eV energy. The particle starts at  $\xi_x = 3L/4$  and  $\xi_y = L/4$  and hits the boundary at  $x = L/2$  and  $y = 0$ . To make the small reflected part of the wave function visible  $|\psi(x, y, t)|$  is drawn. In the usual pictures of  $|\psi(x, y, t)|^2$  reflections would not be visible. Figure 4 shows the dependence of the two-dimensional reflection coefficient  $r$  on the expansion point of the approximation (6). As is seen from Fig. 4 a reflection coefficient less than 1% is easily obtained—even for that relatively small grid. Only a small dependence on the particle energy is observed.

### ACKNOWLEDGMENTS

I would like to thank the "Deutsche Forschungsgemeinschaft" for financial support. I would also like to thank Dr. P. Selbmann, who has brought my attention to the problem.

<sup>1</sup>A. Goldberg, H. M. Schey, and J. I. Schwartz, Am. J. Phys. **35**, 177 (1967).

<sup>2</sup>I. Galbraith, Y. S. Ching, and E. Abraham, Am. J. Phys. **52**, 60 (1984).

<sup>3</sup>W. Frenley, Rev. Mod. Phys. **62**, 745 (1990).

<sup>4</sup>T. Shibata, Phys. Rev. B **43**, 6760 (1991).

<sup>5</sup>B. Engquist and A. Majda, Math. Comput. **31**, 629 (1977).